Research Article

Leru Luo and Changchun Bao*

Braking and attitude control of lunar lander in active descent stage

https://doi.org/10.1515/astro-2022-0217 received November 19, 2022; accepted January 24, 2023

Abstract: China officially launched the lunar exploration project, named "Chang'e Project," in 2004. Then, in 2013, Chang'e-3 completed the soft landing on the lunar surface, starting a series of studies on the soft landing of spacecraft. This study aims to optimize the dynamic flight guidance and attitude control of the lunar landing module represented by Chang'e-3 in the soft landing stage. After analyzing the attitude control requirements of the soft landing stage of the lunar landing module, this study designs the lunar soft landing process under a variable structure sliding mode (VSSM) control. The study also analyzes the influence of the pulse width modulator (PWM) on the soft landing process. The simulation model of the lunar soft landing guidance and control system is established by MATLAB/Simulink, and the traditional proportionalintegral-derivative (PID) control mode is compared with the interference condition. Results show that VSSM + PWM is superior to PID in robustness and accuracy and has a theoretical reference value for future lunar landing exploration and even Mars landing exploration.

Keywords: variable structure sliding mode control, pulse width modulator, lunar soft landing, active descent braking

1 Introduction

Driven by the substantial benefits of lunar exploration, countries globally have issued their own lunar exploration plans, which once again sets off a climax of lunar exploration.

As the shortest extrasolar celestial body from Earth, the moon has become the first target of human exploration activities in deep space (Johnson and Montgomery 2020). As early as 1959, the "Luna 2" unmanned lunar probe was successfully launched from the Soviet Union and finally landed on the lunar surface. Subsequently, the "Cosmos" and "Zond" lunar unmanned exploration activities were successfully carried out. At the same time, a large number of lunar unmanned exploration programs have also emerged in the United States, including "Pioneer," "Ranger," "Lunar Orbiter," "Surveyor," "Explorer," and "Lunar Prospector". During these six soft landing missions and a series of other lunar exploration missions, a large number of lunar soil samples were collected, and scientists analyzed them to obtain a large amount of valuable scientific data. From July 1969 to December 1972, the United States also implemented the "Apollo" manned lunar landing program. The program succeeded totally six times, and also carried out experiments and explorations on soil mechanical properties, meteorology, moonquakes, heat flow, lunar surface, and lunar magnetic field and solar wind, and obtained rich scientific data and brought back about 400 kg of lunar rock samples. The entire "Apollo" mission is of great scientific and historical significance, and the landing of extraterrestrial objects by humans was achieved for the first time. In recent years, the "Clementine" lunar probe has discovered the possible presence of water ice near Antarctica, and the existence of a series of major scientific discoveries has triggered a new wave of lunar exploration around the world. In 2004, the United States proposed the "New Flourishing Plan," two of which are to implement manned missions to return to the moon in 2020 and 2030, respectively, and to achieve manned landing on Mars. In the same year, ESA officially announced the "Goddess of Dawn" super-large interstellar exploration program, and proposed to achieve a manned landing on the moon around 2024, so that human beings can explore and accumulate planet-related survival knowledge and experience on every asteroid outside the earth. In 2005, Japan also proposed a long-term space plan, including the establishment of a lunar base around 2025. In April 2006, a 25 year manned space program was proposed in Russia, and a lunar probe was proposed to be launched in 2015 for a manned lunar mission. In recent years, India has begun to implement the "first lunar flight"

^{*} Corresponding author: Changchun Bao, Aviation College,
Department of Aviation Engineering, Inner Mongolia University of
Technology, Hohhot 010051, China, e-mail: changchun@imut.edu.cn
Leru Luo: College of Science, Inner Mongolia University of
Technology, Hohhot 010051, China

exploration plan, and at the same time, manned lunar exploration programs and Mars exploration programs have also been put on the agenda.

In December 2012, China's Chang'e-2 lunar probe successfully carried out the flying over exploration of asteroid Toutatis. In December 2013, the Chang'e-3 lunar probe realized the first soft landing of Chinese spacecraft on extraterrestrial objects and completed the inspection and exploration of the lunar surface. In November 2014, the reentry and return flight test of phase III of the lunar exploration project was a complete success. This event indicates that China has fully mastered the key technology of spacecraft reentry and returned at speed close to the second universe, which was launched on November 24, 2020. After a 23 day mission cycle, the Chang'e-5 lunar probe returner successfully landed in the predetermined area of Siziwang Banner, Inner Mongolia on December 17, realizing the sampling and return of extraterrestrial objects in China for the first time (Ye 2021).

Through the implementation of the lunar exploration engineering mission, China has obtained a high-resolution all-Moon image map and a high-definition image of the Hongwan area (The State Council Information Office of the People's Republic of China 2016). China also carried out research on lunar morphology, lunar structure, lunar surface material composition, lunar surface environment, and near lunar space environment, including lunar-based astronomical observation.

Landing on the Moon is of two kinds: hard and soft landing (Wang 2021). The former means that when the probe approaches the Moon, it directly impacts the Moon without using the braking device to slow down. The latter requires a detector to turn on the braking system at a certain height from the lunar surface, and uses a small thrust engine to control the detector's speed to the Moon within a very small range, usually a few meters per second. Evidently, considering the scientific research, such as sampling and landing on the Moon, the scientific value of the probe's soft landing is greater than that of the hard landing. In recent years, scholars at home and abroad studied the guidance and control of lunar soft landing, and achieved some research results. Literature proposed to combine the linear-quadratic regulator control algorithm and Aho-Corasick algorithm with the improved particle swarm optimization algorithm (Wang 2020). Literature (Li et al. 2020) improved the accuracy of lander position and velocity estimation through landmark image navigation and beacon navigation technology. The attitude control is completed by rate control attitude hold through the attitude control handle (Duda et al. 2009). The target angular velocity command is generated

by the deflection of the attitude control handle in the pitch and yaw directions. Moreover, the automatic control system tracks the angular velocity command. When the handle returns to zero, the attitude is maintained based on the current attitude. However, these research results are mainly based on the plane model or three degrees of freedom model of the lander. Research mainly focused on the design selection and tracking control of the trajectory of the lander. The attitude control of the lander adopts proportional—integral—derivative (PID) or high-order PID control, and there is still room for improvement in robustness and accuracy.

In this study, a common sliding mode control system in the attitude control system is adopted, in which the variable structure sliding mode (VSSM) control is very suitable for the control process of lunar soft landing. The basic idea of VSSM control is to use different control laws in different regions of the system state space to force the system to move according to the state trajectory of the predetermined sliding mode (Duda et al. 2009, Zhang et al. 2014). The change in structure is realized based on the instantaneous value of trajectory parameters according to the preset switching logic. The biggest difference between VSSM control and other systems is that the control system will change with the state of the system. The VSSM control has the advantages of fast response, independent of parameters, no system online identification, and easy physical implementation. However, as the state will shuttle back and forth near the control surface, it is prone to high-frequency chattering (Duda et al. 2009).

Aiming at the chattering problem, referring to the method of the variable structure PID and pulse demodulator adopted by the "Chang'e-3" detector (Ming et al. 2017), a method of VSSM control combined with pulse demodulator is designed in this study. Pulse width modulator (PWM) is a technology that compares the analog input signal with the signal level of the carrier signal inside the modulator and modulates it into a pulse signal in the form of on/off. As a widely used power electronic device today (Hu and Zhuang 2016, Yang et al. 2014, Zhang et al. 2014), PWM has been a research hotspot, with the advantages of sinusoidal grid-side current, high-power factor, bidirectional energy flow, and adjustable DC voltage compared to various rectifier systems. With the increase in the research on PWM rectified control, some control strategies with excellent performance have been produced (Chen and Joos 2008). Among which, sliding mode control system combining PWM has received widespread attention because of its good dynamic and steady state performance.

This study will comprehensively consider the guidance and attitude of robust control in the process of lunar soft landing. When stabilizing the lander in a certain speed range, with reference to the "Chang'e-3" probe, the attitude is also stabilized in the expected range using VSSM control and pulse demodulator.

This study is further organized as follows. Section 1 introduces the dynamic equation of the lunar lander. Section 2 gives the robust scheme of attitude control, including the design of PWM, VSSM controller, and ignition logic. Section 3 gives a simulation example to verify the effectiveness of the proposed scheme. Section 4 concludes the study.

2 Dynamic equation of lunar soft lander

This section introduces the dynamic equations of the lunar lander. First, two coordinate systems of the soft lander are defined, and then the attitude dynamic model of the lander is given.

2.1 Introduction to the coordinate system

The dynamic equation of lunar soft landing is related to two coordinate systems. The lunar-centered inertial (LCI) frame is defined as: the origin O_1 is selected at the lunar center, the O_1X_1 axis points to the starting point of dynamic descent, the O_1Y_1 axis is perpendicular to the O_1X_1 axis and points to the direction of the landing point, and the O_1Z_1 axis direction is determined according to the right-hand rule.

The lander body frame is defined as follows: the origin O_b is the detector, the O_bX_b axis coincides with the vector direction from the lunar center to the detector centroid, the direction away from the lunar center is positive, the O_bY_b axis perpendicular to the O_bX_b axis that

points to the motion direction is positive, and O_bZ_b is determined according to the right-hand rule.

The direction of the braking thrust coincides with the body axis of the lander (Figure 1).

The rotational angular velocity of the Moon is very small (Zhang and Duan 2013), and the soft landing process is very short, generally within a few minutes to tens of minutes. Thus, the rotational angular velocity of the Moon can be ignored when designing the guidance and control systems. In the lunar surface solid coordinate system, we suppose that $\mathbf{r} = [r_x, r_y, r_z]^T \in \mathbb{R}^3$ is the position vector of the aircraft, $\mathbf{v} = [v_x, v_y, v_z]^T \in \mathbb{R}^3$ is the velocity vector of the aircraft, $F = [F_x, F_y, F_z]^T \in \mathbb{R}^3$ is the thrust vector, and $R_{\rm m}$ is the vector pointing from the center of the Moon $O_{\rm I}$ to the landing point $O_{\rm b}$. Then, the dynamic equation of the centroid motion under the solid connection of the lunar surface is as follows (Sidi 1997):

$$\begin{cases}
\dot{r}_{x} = v_{x}, \\
\dot{r}_{y} = v_{y}, \\
\dot{r}_{z} = v_{z}, \\
\dot{v}_{x} = -\frac{\mu}{\|R_{m} + \mathbf{r}\|^{3}} (r_{x} + R_{m}) + a_{x}, \\
\dot{v}_{y} = -\frac{\mu}{\|R_{m} + \mathbf{r}\|^{3}} r_{y} + a_{y}, \\
\dot{v}_{z} = -\frac{\mu}{\|R_{m} + \mathbf{r}\|^{3}} r_{z} + a_{z},
\end{cases}$$
(1)

where μ is the gravitational constant of the Moon, $R_{\rm m}$ = $||R_m||$, and its subscript m is the quality of the aircraft, and \dot{r}_x , \dot{r}_y , \dot{r}_z , \dot{v}_x , \dot{v}_y , \dot{v}_z are derivatives to time t of r_x , r_y , r_z and v_x , v_y , v_z .

To obtain the attitude of the lunar lander, we suppose that the lander body frame can be rotated to the LCI frame about $Z_b - Y_b - X_b$. Then, we can define ψ , θ , and γ as the angles of body frame rotating about Z_b , Y_b , and X_b . Defining the rotational angular velocity of the body coordinate system as $\omega = [\omega_x, \omega_y, \omega_z]^T \in \mathbb{R}^3$, the attitude of flight motion equations is as follows (Zhang and Duan 2013):

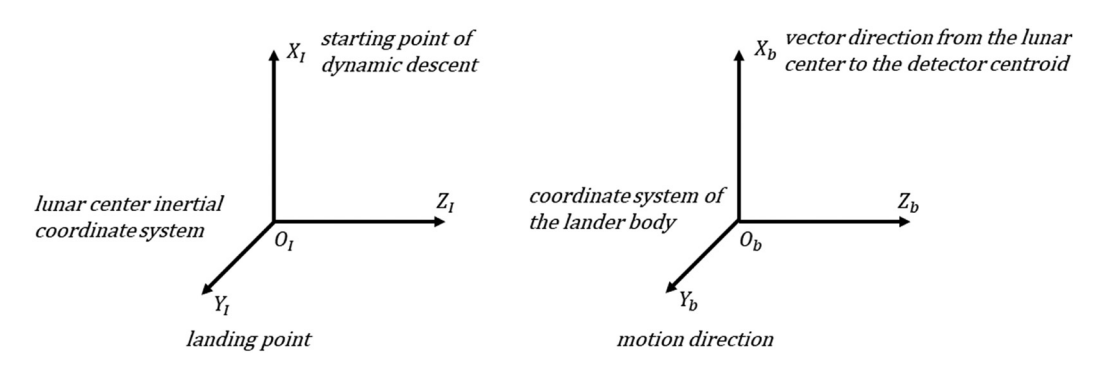


Figure 1: Coordinate systems.

$$\begin{cases} \dot{y} = \omega_{x} + \omega_{y} \tan \theta \sin y + \omega_{z} \tan \theta \cos y, \\ \dot{\theta} = \omega_{y} \cos y - \omega_{z} \sin y, \\ \dot{\psi} = \omega_{y} \frac{\sin y}{\cos \theta} + \omega_{z} \frac{\cos y}{\cos \theta}. \end{cases}$$
(2)

The attitude dynamics equation is as follows:

$$I\omega + \omega \times I\omega = M, \tag{3}$$

where $\mathbf{M} = [M_x, M_y, M_z]^T$ is the control torque vector. Suppose the moment of inertia matrix is

$$I = \begin{bmatrix} I_x & & & \\ & I_y & & \\ & & I_z \end{bmatrix}$$
.

Let $L_x = (I_y - I_z)/I_x$, $L_y = (I_z - I_x)/I_y$, $L_z = (I_x - I_y)/I_z$, then, attitude dynamics equation can be transformed into

$$\begin{cases} \dot{\omega}_{x} = L_{x}\omega_{y}\omega_{z} + \frac{M_{x}}{I_{x}}, \\ \dot{\omega}_{y} = L_{y}\omega_{x}\omega_{z} + \frac{M_{y}}{I_{y}}, \\ \dot{\omega}_{z} = L_{z}\omega_{x}\omega_{y} + \frac{M_{z}}{I_{z}}. \end{cases}$$

$$(4)$$

Suppose that the attitude control system of the aircraft is provided by the reaction controller in the direction of the three inertia axes, the thrust is provided by the engine mounted at the bottom of the aircraft. In addition, the engine is fixed to the aircraft, and the thrust direction coincides with the $X_{\rm b}$ axis, providing only the thrust along the box direction. Then, the thrust in the lander body frame is expressed as follows:

$$F = [F, 0, 0]^T$$

where F = ||F||. Evidently, the control of thrust over the centroid motion of the vehicle relies on the attitude angle of the aircraft, which can be obtained by projecting the thrust vector F into the lunar solid connection.

$$\begin{bmatrix} F_x \\ F_y \\ F_z \end{bmatrix} = T \begin{bmatrix} F \\ 0 \\ 0 \end{bmatrix} = \begin{bmatrix} F\cos\theta\cos\psi \\ F\cos\theta\sin\psi \\ -F\sin\theta \end{bmatrix}, \tag{5}$$

where T is the transform matrix between the ECI frame and lander body frame.

$$T = \begin{bmatrix} \cos\theta\cos\psi & \cos\theta\sin\psi & -\sin\theta \\ -\cos y\sin\psi & \cos y\cos\psi & \cos\theta\sin\gamma \\ +\sin\theta\sin y\cos\psi & +\sin\theta\sin\psi\sin\gamma \\ \sin y\sin\psi & -\sin y\cos\psi & \cos\theta\cos\gamma \\ +\sin\theta\cos y\cos\psi & +\sin\theta\sin\psi\cos\gamma \end{bmatrix}.$$

Based on Newton's second law, replace the force in Eq. (5) with acceleration and take the numeric value in the acceleration sequence into Eq. (1), the complete coupled kinetic equations can then be obtained by combining the results and Eqs. (4) and (2) as follows:

$$\begin{cases}
\dot{r}_{x} = v_{x}, \dot{r}_{y} = v_{y}, \dot{r}_{z} = v_{z}, \\
\dot{v}_{x} = -\frac{\mu}{\|\mathbf{R}_{m} + \mathbf{r}\|^{3}} (r_{x} + R) + \frac{F\cos\theta\cos\psi}{m}, \\
\dot{v}_{y} = -\frac{\mu}{\|\mathbf{R}_{m} + \mathbf{r}\|^{3}} r_{y} + \frac{F\cos\theta\sin\psi}{m}, \\
\dot{v}_{z} = -\frac{\mu}{\|\mathbf{R}_{m} + \mathbf{r}\|^{3}} r_{z} - \frac{F\sin\theta}{m}, \\
\dot{y} = \omega_{x} + \omega_{y}\tan\theta\sin\gamma + \omega_{z}\tan\theta\cos\gamma, \\
\dot{\theta} = \omega_{y}\cos\gamma - \omega_{z}\sin\gamma, \\
\dot{\theta} = \omega_{y}\cos\gamma - \omega_{z}\sin\gamma, \\
\dot{\psi} = \omega_{y}\frac{\sin\gamma}{\cos\theta} + \omega_{z}\frac{\cos\gamma}{\cos\theta}, \\
\dot{\omega}_{x} = L_{x}\omega_{y}\omega_{z} + \frac{M_{x}}{I_{x}}, \\
\dot{\omega}_{y} = L_{y}\omega_{x}\omega_{z} + \frac{M_{y}}{I_{y}}, \\
\dot{\omega}_{z} = L_{z}\omega_{x}\omega_{y} + \frac{M_{z}}{I_{z}}.
\end{cases}$$
(6)

Furthermore, we need to consider the changes in the mass of the aircraft and supplement the mass change equation as follows:

$$\dot{m} = -\frac{F}{I_{\rm sp}g_0},\tag{7}$$

where $I_{\rm sp}$ is the specific impulse of the engine; and g_0 is the gravitational acceleration at the Earth's Sea level (Ming *et al.* 2017). Without loss of universality, we assume that moment of inertia I_x , I_y , I_z is proportional to the mass of the aircraft individually.

As the main engine is fixed to the bottom of the aircraft, the change in attitude angle directly affects the projection component of thrust on the three coordinate axes of the lunar solid connection. Evidently, orbital dynamics rely on attitude dynamics, and a more serious coupling exists between them.

2.2 Attitude model of lunar lander

The attitude control scheme of lunar soft lander adopts the VSSM + PWM control method. According to previous studies, we choose the method of controlling the attitude direction by solving the coupling of thrust direction, roll and yaw angles. The control law is designed as follows: First, the model is transformed as follows:

$$\mathbf{x} = [x_1, x_2, x_3, x_4, x_5, x_6]^T = [y, \dot{y}, \theta, \dot{\theta}, \psi, \dot{\psi}]^T.$$

Then, the attitude model can be rewritten as follows (Zhang *et al.* 2014):

$$\dot{x}_{1} = x_{2}
\dot{x}_{2} = \frac{1}{I_{x}} M_{x} + \left(-\frac{(I_{z} - I_{y})}{I_{x}} k_{z} k_{y} + \frac{k_{y} \sin y + k_{z} \cos y}{\cos^{2} y} \dot{\psi} \right)
+ \tan \psi \left(\dot{k}_{y} \sin y + k_{y} \cos y \right)
+ \dot{k}_{z} \cos y - k_{z} \sin \dot{y} \right),
\dot{x}_{3} = x_{4},
\dot{x}_{4} = \frac{1}{I_{y}} M_{y} \cos y + \left(-\frac{(I_{x} - I_{z})}{I_{y}} k_{z} k_{x} \cos y - k_{y} \dot{y} \sin y - \dot{k}_{z} \sin y - k_{z} \dot{y} \sin y \right),
\dot{x}_{5} = x_{6},
\dot{x}_{6} = \frac{1}{I_{z}} M_{z} \frac{\cos y}{\cos \theta} + \left(-\frac{(I_{y} - I_{x})}{I_{z}} k_{y} k_{x} + \frac{\cos y}{\cos \psi} + \frac{\sin y}{\cos \psi} + \dot{k}_{y} \right)
+ \frac{k_{y} \cos y - k_{z} \sin y}{\cos \psi} \dot{y} + \frac{(k_{y} \cos y + k_{z} \sin y) \sin \psi}{\cos^{2} \psi} \right).$$
(8)

3 Attitude control scheme of lunar soft lander

This section presents the attitude control scheme of lunar soft lander. First, the PWM is designed, the second section

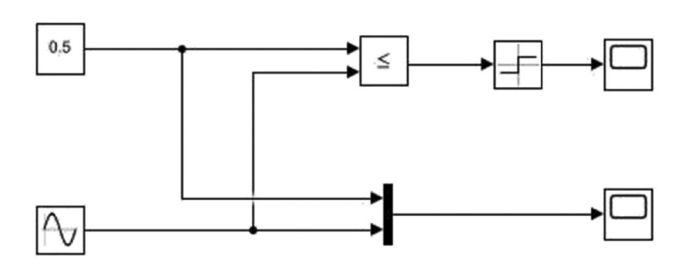


Figure 2: Structure of PWM.

gives the design of VSSM controller, and the third section gives the design of ignition logic.

3.1 Theoretical basis

Figure 2 shows the structure of the PWM.

For the time output by the attitude controller of the lunar lander ground test model, the continuous (+) and (-) control inputs will be input into the PWM, which needs to output them as (+) pulse signal and (-) pulse signal. Generally, PWM can only output the (+) pulse signal, so the (-) pulse signal output is designed for the lunar lander ground test model. The diagram shows that the designed PWM modulates the continuous signal into (+) pulse signal or (-) pulse signal and outputs it. After comparing the VSSM control proposed in the literature with the PID + PWM method adopted by Chang'e-3, a VSSM + PWM method is proposed in this study (Figure 3).

3.2 Design of the variable structure attitude control system

First, the sliding mode surface is designed. We suppose the initial attitude of the lander to be γ_0 , θ_0 , and ψ_0 . Then, we can set the desired attitude angle and attitude angular velocity as follows:

$$\mathbf{x}_{d} = [x_{d1}, x_{d2}, x_{d3}, x_{d4}, x_{d5}, x_{d6}]^{T} = [y_{d}, \dot{y}_{d}, \theta_{d}, \dot{\theta}_{d}, \psi_{d}, \dot{\psi}_{d}]^{T}$$
$$= [y_{0} \mp 1^{\circ}, 0, \theta_{0} \mp 1^{\circ}, 0, \psi_{0} \mp 1^{\circ}, 0]^{T}.$$

Taking the deviation between the actual value and the expected value

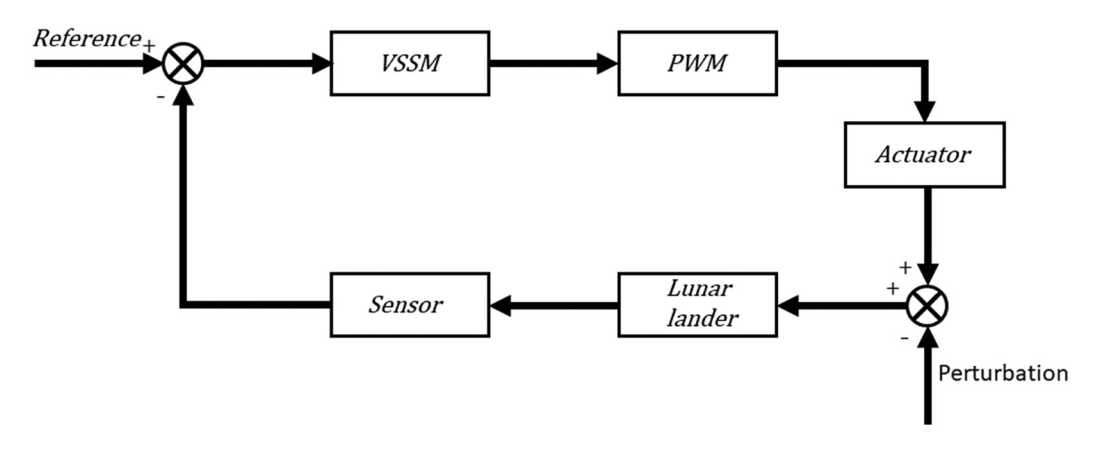


Figure 3: Soft landing control system.

$$\mathbf{e} = [e_1, e_2, e_3, e_4, e_5, e_6]^T$$

$$= [(x_1 - x_{d1}), (x_2 - x_{d2}), (x_3 - x_{d3}), (x_4 - x_{d4}), (x_5, -x_{d5}), (x_6 - x_{d6}),]^T$$

Then, the linear sliding mode surface is as follows:

$$\begin{cases} S_x = K_x e_1 + e_2 = K_x (y - y_d) + (\dot{y} - \dot{y}_d), \\ S_y = K_y e_3 + e_4 = K_y (\theta - \theta_d) + (\dot{\theta} - \dot{\theta}_d), \\ S_z = K_z e_5 + e_6 = K_z (\psi - \psi_d) + (\dot{\psi} - \dot{\psi}_d), \end{cases}$$
(9)

where K_x , K_v , and K_z are the parameters to be designed.

Next the variable structure *c*ontroller is designed by the Lyapunov backstepping method.

To facilitate derivation, the following vectors are designed:

Control vector

$$\mathbf{u} = [M_x, M_y, M_z,]^T$$
.

Control gain matrices

$$b(\mathbf{x},t) = \begin{bmatrix} \frac{1}{I_x} & 0 & 0\\ 0 & \frac{\cos y}{I_y} & 0\\ 0 & 0 & \frac{\cos y}{I_x \cos \theta} \end{bmatrix},$$

$$f(\mathbf{x}, t) = [f_1(\mathbf{x}, t), f_2(\mathbf{x}, t), f_3(\mathbf{x}, t)],$$

where

$$\begin{cases} f_{1}(\boldsymbol{x},t) = -\frac{(I_{z} - I_{y})}{I_{x}} k_{z} k_{y} + \frac{k_{y} \sin y + k_{z} \cos y}{\cos^{2} \theta} \dot{\theta} \\ + \tan \theta (\dot{k}_{y} \sin y + k_{y} \cos y + \dot{k}_{z} \cos y - k_{z} \sin \dot{y}) \end{cases}$$

$$f_{2}(\boldsymbol{x},t) = -\frac{(I_{x} - I_{z})}{I_{y}} k_{z} k_{x} \cos y - k_{y} \dot{y} \sin y - \dot{k}_{z} \sin y$$

$$- k_{z} \dot{y} \sin y,$$

$$f_{3}(\boldsymbol{x},t) = -\frac{(I_{y} - I_{x})}{I_{z}} k_{y} k_{x} + \frac{\cos y}{\cos \psi} + \frac{\sin y}{\cos \psi} + \dot{k}_{y}$$

$$+ \frac{k_{y} \cos y - k_{z} \sin y}{\cos \psi} \dot{y} + \frac{(k_{y} \cos y + k_{z} \sin y) \sin \psi}{\cos^{2} \psi}$$

Output vector

$$y = [x_1, x_3, x_5,]^T$$
.

Error matrix

$$E = [e_1, e_3, e_5, e_2, e_4, e_6]^T$$
.

The attitude control equation is changed to

$$\begin{cases} \dot{y} = z \\ \dot{z} = \mathbf{f}(\mathbf{x}, t) + \Delta \mathbf{f}(\mathbf{x}, t) + b(\mathbf{x}, t)\mathbf{u} + \mathbf{d}(t) \end{cases}$$
(10)

The sliding surface can be rewritten as

$$S(\mathbf{x}, t) = CE$$

$$C = [C_1, C_2],$$

 $C_1 = \text{diag}(c_1, c_2, c_3),$
 $C_2 = \text{diag}(c_4, c_5, c_6),$

where *C* is the control gain matrix to be designed. We then take the Lyapunov function as

$$V = \frac{1}{2}S^T S. \tag{11}$$

The differentiation of Eq. (11) is

$$\dot{V} = S^{T} \dot{S} = S^{T} C_{2} [f(\mathbf{x}, t) - \ddot{\mathbf{x}}_{1d}] + S^{T} C_{2} b(\mathbf{x}, t) \mathbf{u}
+ S^{T} C_{2} [\Delta f(\mathbf{x}, t) + \mathbf{d}(t)] + C_{1} \dot{E}
\leq S^{T} C_{2} [f(\mathbf{x}, t) - \ddot{\mathbf{x}}_{1d}] + S^{T} C_{2} b(\mathbf{x}, t) \mathbf{u} + C_{1} \dot{E}
+ ||S^{T} C_{3}|| ||\Delta f(\mathbf{x}, t) + \mathbf{d}(t)||.$$
(12)

Without loss of generality, we assume that system uncertainty $\Delta f(x, t)$ and external disturbance d(t) have the following properties:

$$\|\Delta f(x, t)\| \le F', \|d(t)\| \le D.$$

Then, the control input can be rewritten as follows:

$$u(t) = -b(x, t)^{-1} [f(x, t) - \ddot{x}_{1d} + C_2^{-1}C_1\dot{E}]$$

$$-b(x, t)^{-1} \frac{C_2^T S}{\|C_2^T S\|} [F' + D + A],$$
(13)

where $A = [a_x, a_y, a_z]$ is the gain matrix to be designed. Substituting Eq. (13) in Eq. (12), we can get

$$\dot{V} = \|C_2^T S\| \|\Delta f(x, t) + d(t)\| - [F' + D + A] \|C_2^T S\|
\leq \|C_2^T S\| \|\Delta f(x, t)\| - F' + \|d(t) - D\| - A \|C_2^T S\| < 0.$$
(14)

From the above formula, the system is Lyapunov stable. Considering the inherent defects of sliding mode control and the chattering caused by high-frequency switching operation, the boundary layer continuity method is selected to eliminate the chattering, that is, the boundary layer is introduced near the sliding surface S = O, and the reaching law of saturation function is adopted (Li *et al.* 2020):

$$\begin{cases} K_{x}(\gamma - \gamma_{d}) + (\dot{\gamma} - \dot{\gamma}_{d}) = -\frac{a_{x}S_{x}}{|S_{x}| + X_{x}} - l_{x}S_{x}, \\ K_{y}(\theta - \theta_{d}) + (\dot{\theta} - \dot{\theta}_{d}) = -\frac{a_{y}S_{y}}{|S_{y}| + X_{y}} - l_{y}S_{y}, \\ K_{z}(\psi - \psi_{d}) + (\dot{\psi} - \dot{\psi}_{d}) = -\frac{a_{z}S_{z}}{|S_{z}| + X_{z}} - l_{z}S_{z}, \end{cases}$$
(15)

where a_x , a_y , a_z , l_x , l_y , l_z are the constants to be designed.

In the sliding mode variable structure control, the control input should be able to force the system state from any initial point to the sliding mode, and keep it stable and reliable in the sliding mode. According to Lyapunov function (14), the sliding mode control of the

system is insensitive to the uncertainties such as parameters and disturbances, that is, it has strong robustness. The sliding mode surface (15) of the variable structure controller designed in this study is a linear time-varying sliding mode surface, which makes the state of the system lie on the sliding mode surface at the beginning, eliminating the arrival stage of the sliding mode, to ensure the global robustness and stability of the system.

3.3 Ignition logic

During the flight of the landing module, after calculating the expected control torque, the attitude control system controls the ignition logic and ignition time of the attitude control engine to generate the actual control torque

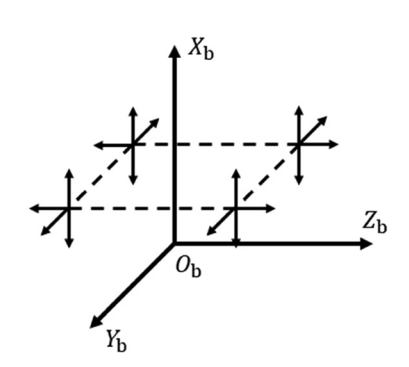


Figure 4: Configuration mode of attitude control engine.

(Duda *et al.* 2009). The attitude control engine system of the lander, referring to the Chang'e-3 detector, adopts 16 pulse engines to form four independent and structurally identical subsystems. Each subsystem is divided into four groups, which are, respectively, installed around the detector. Moreover, to realize the three-axis control of the center of mass, the geometric center formed by the four groups of pulse engines shall coincide with the center of mass of the detector in the hovering stage. When the attitude control engine system adjusts and controls the attitude, to avoid the influence of the generated thrust on the center of mass, the pulse engine should work in pairs. Figure 4 shows the configuration mode of the attitude control engine (Zhang *et al.* 2014).

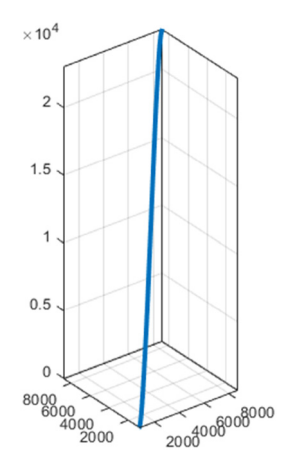


Figure 6: Three-dimensional trajectory of the VSSM + PWM lander.

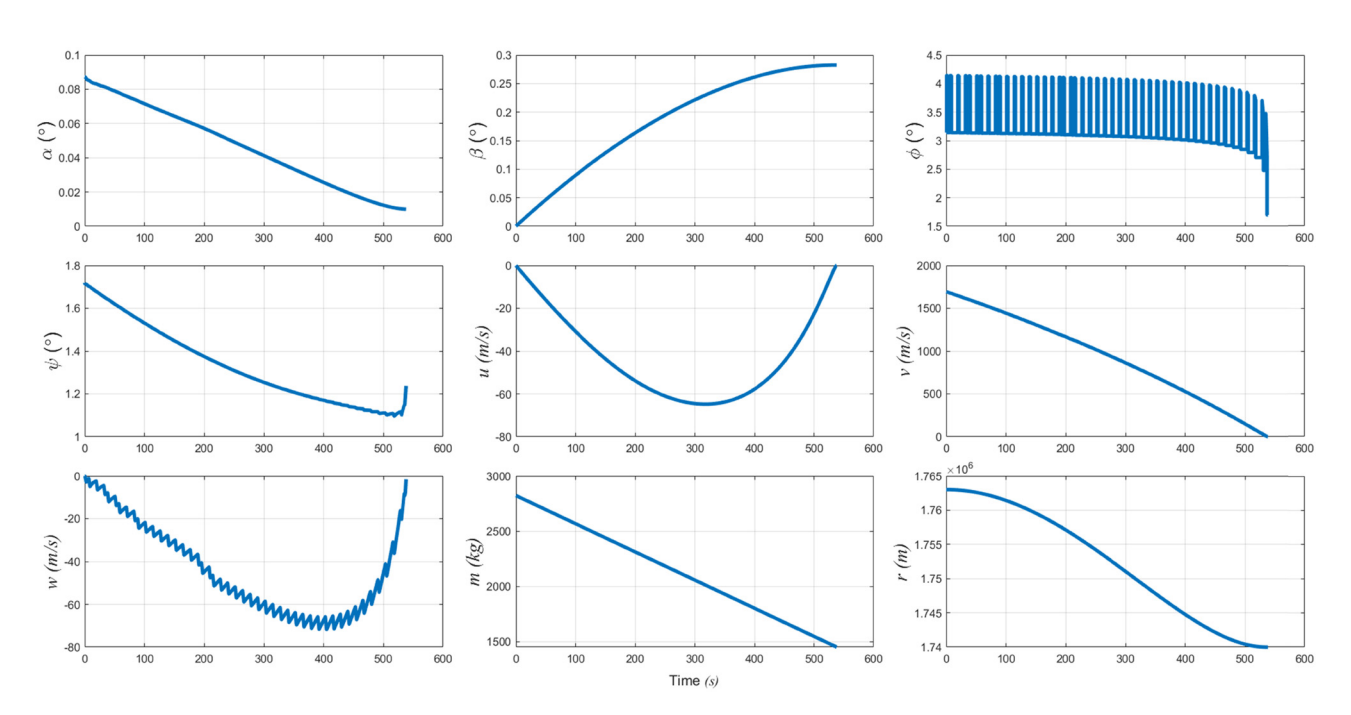


Figure 5: Latitude, longitude, attitude angle, velocities, and distance of the VSSM + PWM lander.

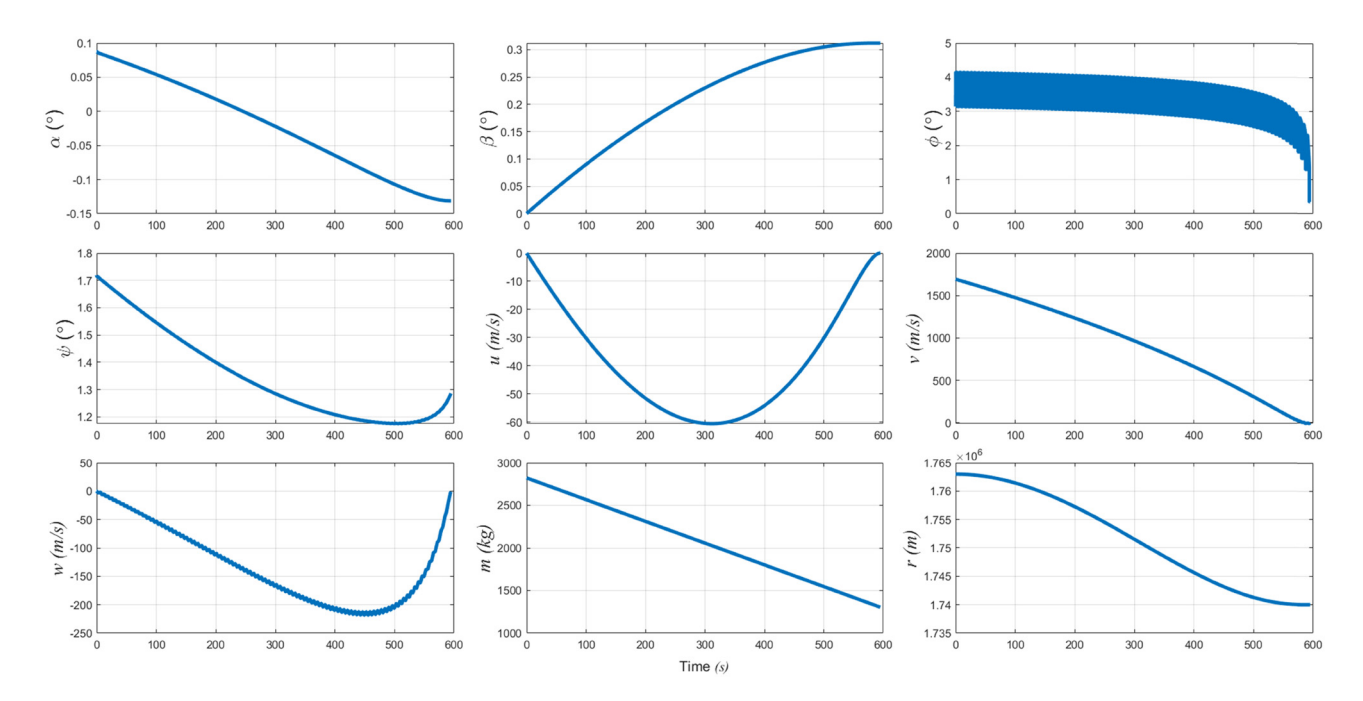


Figure 7: Latitude, longitude, attitude angle, velocities, and distance of the PID + PWM lander.

4 Simulation

This section gives a simulation example to verify the effectiveness of the proposed scheme (Figures 5–7).

4.1 Simulation parameters

Parameters	Values
Lunar gravi- tational	$\mu = 4.88775 \times 10^{12} \text{ m}^3/\text{s}^2$
constant Lunar radius	$R_{\rm I} = 1,738 \text{km}$
Simulation parameters of	$r_0 = 1,753 \text{ km}, \ \alpha_0 = 0.27399^\circ, \ m_0 = 2,822 \text{ kg}$
the lander	
Initial veloci- ties of the	$u_0 = 0$, $v_0 = 1,692$ m/s, $w_0 = 0$
lander	
Expected simulation results	$r_f = 1,740 \text{ km}, u_f = w_f = 0, v_f = 3 \text{ m/s}$
	$F = 7,500 \text{ N}, I_{\text{sp}} = 300 \text{ s}, g_E = 9.80665 \text{ m/s}^2$
Attitude con-	$F_E = 150 \text{ N}$
trol engine	_
thrust	
Disturbance torque before	$d_x = d_y = d_z = 0.5 + 0.5\sin(t)(N)$

```
PWM modulation PID controller for comparison (Yang et al. 2014) \begin{cases} y_d = -\arcsin[K_p(u_d-u) + K_d(\dot{u}_d-\dot{u})] \\ \psi_d = \arcsin[K_p(v_d-v) + K_d(\dot{v}_d-\dot{v})] \end{cases}
```

4.2 Simulation results

The simulation results show that under the same simulation environment, the VSSM + PWM controller reached the specified height of the lunar surface at the speed of 1.3143 m/s at 538.835 s, and the attitude angle is within 1°. Compared with the adjustment time of 685 s and the adjustment error of Chang'e-3, the VSSM + PWM controller meets the control requirements and the performance is improved, whereas the PID + PWM controller reached the specified altitude and the expected speed at 594.997 s. VSSM + PWM for the complex coupling model is better than PID + PWM in terms of accuracy and convergence.

According to the above simulation results, the lunar soft landing model can describe the dynamic characteristics of the lander in detail. However, given the underactuated and strong coupling characteristics of the lander, designing a nonlinear controller into a nonlinear model is difficult. Given the design difficulties described above, this study first transforms the complex nonlinear lander

model into a linear lander model through the linearization method, and designs the linear control theory. Second, the VSSM controller is selected owing to its strong robustness. For the actual lander system, considering the factors such as rounding error, parameter drift, aging of controller equipment and limited word length in the digital system in the numerical algorithm, the predetermined control performance of the closed-loop system will decline without the robust controller. Under the VSSM + PWM controller, the states of the lander tend to expected values quickly and smoothly, and the closed-loop error system has the expected control performance. Third, all the assumptions proposed in this study meet the actual lander system. Interference is ubiquitous during the lunar landing. Taking the lunar environmental disturbance as an example, the lunar environmental disturbance can be divided into different types: lunar dust (lunar soil) disturbance, ultra-high vacuum environment, additional ultraviolet radiation, alternating thermal cycle, and others. They will produce many different types of disturbances. Therefore, the anti-interference control method proposed in this study is effective for the actual lander system. In addition, the feedback signal used by the controller can be used for the actual landing of the lander. The designed VSSM + PWM lander system is reasonable. Finally, time-varying disturbances and unmeasurable states always exist in the landing process. Establishing a pulse modulator to estimate the disturbances is feasible. Based on the above considerations, the main research results of this study have a certain reference value for the actual landing attitude control system.

5 Conclusion

This study presents a design of a guidance loop and attitude control system for the dynamic descent phase of the lunar soft landing. After investigating the Chang'e-3 and Chang'e-5, an attitude control system based on VSSM control theory is proposed. Without complex data analysis of the system, the expected control torque is obtained according to the deviation between the actual attitude angle and the expected attitude angle. Combined with the PWM successfully used by the Chang'e-3 detector, the ignition logic of the attitude control engine is accurately controlled. The simulation results show that when the dynamic model error and environmental interference are bounded, the VSSM attitude control lunar landing system combined with PWM has the following advantages: (i) the VSSM attitude control lunar landing system combined

with PWM can effectively suppress external interference with good global robustness; (ii) compared with PID combined with PWM adopted by Chang'e-3 detector, the attitude control system has evident advantages in terms of speed and accuracy; (iii) the lunar landing system of the attitude control system greatly saves the propellant consumed by attitude control and the whole landing time. Although the attitude control system still has some shortcomings such as chattering, the VSSM attitude control lunar landing system with PWM has high application value in future lunar exploration and even Mars exploration.

Acknowledgements: We gratefully acknowledge the reviewers and editors for their helpful and constructive suggestions that helped us substantially improve the article.

Funding information: This work was supported by the National Natural Science Foundation of China Youth Fund (Grant No. 11902166) and Natural Science Foundation of Inner Mongolia Autonomous Region (Grant No. 2021LHMS01002).

Author contributions: L.L.: conceptualization, methodology, software, validation, data curation, writing-original draft, visualization, and project administration; C.B.: conceptualization, validation, supervision, project administration, and funding acquisition.

Conflict of interest: The authors declare no conflict of interest.

Data availability statement: The data that support the findings of this study are available from the corresponding author upon reasonable request.

References

Chen B, Joos G. 2008. Direct power control of active filters with averaged switching frequency regulation. IEEE Trans Power Electron. 23(6):2729-37.

Duda R, Johnson C, Fill J. 2009. Design and analysis of Lunar lander manual control modes. IEEE Aerospace Conference; 2009 Mar 7-14; Big Sky (MT), USA, IEEE, 2009. p. 1-16.

Hu J, Zhuang K. 2016. Advanced variable structure control theory and application. Xi'an: Northwest University of Technology Press.

Johnson AE, Montgomery JF. 2020. Overview of terrain relative navigation approaches for precise lunar landing. IEEE Aerospace Conference; 2008 Mar 1-8; Big Sky (MT), USA. IEEE, 2008. p. 1-10.

- Li J, Zhang H, Zhang X, Guan Y. 2020. Research on GNC Technology of manned lunar soft landing. Manned spaceflight. 26(6):733-740+750. doi: 10.16329/j.cnki.zrht.2020.06.010.
- Ming X, Yuying L, Tong L, Xin S. 2017. Attitude pointing schemes and spacecraft configurations for liberation-point-orbit spacecraft. Aerosp Sci Technol. 65:1–8.
- Sidi J. 1997. Spacecraft Dynamics and Control: A Practical Engineering Approach. New York: Cambridge University Press.
- The State Council Information Office of the People's Republic of China. 2016. China's Space Activities in 2016. China National Space Administration 1:10–17.
- Wang R. 2021. Flying to focusing on major foreign space activities. Space International. 505(1):45-51.
- Wang F. 2020. Parameter optimization of soft landing trajectory tracking controller of lunar probe. Harbin: Harbin Institute of Technology. doi: 10.27061/d.cnki.ghgdu.2020.001885.

- Yang W, Son J, Lee C. 2014. A study on the path tracking performance of lunar lander demonstrator using a PWM-based thrust controller. J Korean Soc Aviat Aeronaut 22(4):75–80.
- Ye C. 2021. Chang'e-5 mission: the final work of strategic planning of lunar exploration project. J Logist Chinese Organs. 279(3):64-67.
- Zhang F, Duan G. 2013. Integrated translational and rotational control for the terminal landing phase of a lunar module. Aerosp Sci Technol. 27(1):112–126.
- Zhang H, Li J, Guan Y, Huang X. 2014. Autonomous navigation of dynamic descent of Chang'e 3 lander. Control Theory Appl. 31(12):1686–1694.
- Zhang H, Guan Y, Huang X, Li J, Zhao Y, Yu P, et al. 2014. Guidance navigation and control for chang'E-3 powered descent. Sci Tech. 44:377-384. (in Chinese)